Journal of Power Sources 267 (2014) 629–634

Contents lists available at ScienceDirect

Journal of Power Sources

journal homepage: www.elsevier.com/locate/jpowsour

Short communication

High areal capacity, micrometer-scale amorphous Si film anode based on nanostructured Cu foil for Li-ion batteries

Wenping Si [a, b, *], Xiaolei Sun [a, b], Xianghong Liu [a], Lixia Xi [c], Yandong Jia [c], Chenglin Yan [a, d, *], Oliver G. Schmidt [a, b, e, f]

[a] Institute for Integrative Nanosciences, IFW Dresden, Helmholtz Strasse 20, Dresden, 01069, Germany
[b] Material Systems for Nanoelectronics, Chemnitz University of Technology, Reichenhainer Strasse 70, Chemnitz, 09107, Germany
[c] Institute for Complex Materials, IFW Dresden, Helmholtz Strasse 20, Dresden, 01069, Germany
[d] School of Energy, Soochow University, Suzhou, Jiangsu, 215006, China
[e] Center for Advancing Electronics Dresden, Dresden University of Technology, Germany
[f] Merge Technologies for Multifunctional Lightweight Structures, Chemnitz University of Technology, Germany

HIGHLIGHTS

- Nanostructured Cu foil is prepared by anodic oxidation for thick Si film loading.
- Copper oxide nanofibers are in-situ electrochemically reduced to metallic Cu.
- Metallic Cu nanofibers work as matrix for thick Si film.
- The engineered thick Si film anode exhibits a high areal capacity.

GRAPHICAL ABSTRACT

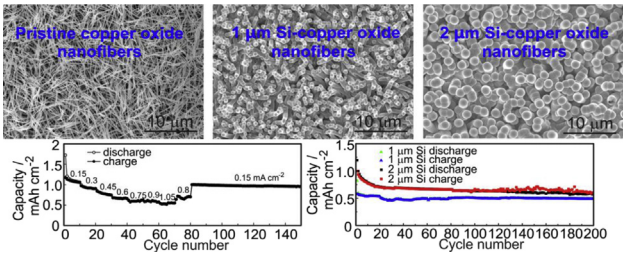

ARTICLE INFO

Article history:
Received 26 March 2014
Received in revised form
17 May 2014
Accepted 27 May 2014
Available online 5 June 2014

Keywords:
Micrometer-scale silicon film
Li-ion battery
High areal capacity
Copper oxide nanofiber
Anode

ABSTRACT

We report a feasible design to fabricate micrometer-scale Si films deposited on nanostructured Cu foil as high areal capacity anodes for Li-ion batteries with excellent cycling performance. Nanostructured copper oxides are prepared by anodic oxidation of Cu foil in alkaline solution. The resultant copper oxide nanofibers function as matrix for thick Si films (1–2 μm) loading. Metallic Cu nanofibers are obtained by in-situ electrochemical reduction at low potentials, which work as electrical highways for fast electron transport and a reliable mechanical matrix to accommodate volume changes during lithium–silicon alloy/dealloy processes. The engineered thick Si film anode exhibit both high areal capacity (0.48 mAh cm^{-2} for 1 μm Si film and 0.6 mAh cm^{-2} for 2 μm Si film after 200 cycles at 0.225 mA cm^{-2}) and excellent rate capability (0.52 mAh cm^{-2} at 1.05 mA cm^{-2} for 2 μm Si film). The 2 μm silicon film electrode is able to recover to the initial value of 1 mAh cm^{-2} when the current rate is set back to 0.15 mA cm^{-2} even after cycling at high current rates. The reported concept can be a general method for high-loading-film electrodes, which is industrial scalable and compatible with current battery manufacturing processes.

1. Introduction

Silicon, as an attractive candidate for Li-ion batteries (LIBs) anodes, has high theoretical capacity (3579 mAh g^{-1} at room temperature for $Li_{3.75}Si$) [1–5], but a very large volume expansion

* Corresponding authors. Institute for Integrative Nanosciences, IFW Dresden, Helmholtz Strasse 20, Dresden, 01069, Germany. Tel.: +49 351 4659 869; fax: +49 351 4659 782.
E-mail addresses: w.si@ifw-dresden.de, siwp86@gmail.com (W. Si), c.yan@ifw-dresden.de (C. Yan).

http://dx.doi.org/10.1016/j.jpowsour.2014.05.136
0378-7753/

(around 280%) [5] of silicon is resulted from alloying with lithium, leading to pulverization and eventual loss of its electrochemical activity. Decreasing the dimension of silicon electrodes and introducing multiphase such as carbon (most promising), Cu, Ti, *etc*. have been demonstrated to be feasible approaches to overcome this issue [6–10]. Various silicon nanostructures such as nanowires [11], nanotubes [12], nanospheres [13], Si/carbon nanocomposites [14–16], including Si/carbon rolled-up membranes [17], were thus fabricated and all showed longer cycling life as candidate anode materials compared with bulk Si, since nanostructures can accommodate large volume change and retain a longer lifetime. Nano-sized silicon particle composites coated with conducting polymer/carbon additives have also received considerable attention as anodes for LIBs [18,19].

Amorphous Si thin film electrodes with 2D nanostructures fabricated by various physical deposition methods also showed improved specific capacity (more than 2000 mAh g^{-1}) and cyclability (over 200 cycles), due to its strong adhesion by the large contact area between the Si film and the current collector [8,20]. But most of the Si films are too thin (≤500 nm) [7,21] to provide enough capacity to match the performance of commercialized cathodes. And Si films at least with thicknesses of several micrometers are desired to obtain sufficient capacity. It is however demonstrated that micrometer-scale Si films (>1 μm) cannot maintain high capacity over long cycling time. For a 1 μm Si film, a reversible capacity of 3000 mAh g^{-1} did not last for more than 12 cycles [1], and for a 1.2 μm Si film, a capacity of 1000 mAh g^{-1} was obtained for the first three cycles but it dropped to 200 mAh g^{-1} after only 20 cycles [22]. One effective strategy to improve the cycling stability is to roughen the surface of the current collector, which enhances the adhesion force of Si films to current collector. Takamura et al. [23] have reported that a 3.6 μm Si film on an electrolytically deposited Cu foil current collector could maintain a capacity of 2000 mAh g^{-1} for about 50 cycles. Yin et al. [24] have succeeded in maintaining a capacity of 0.9 mAh cm^{-2} at 0.1C over 200 cycles for a 2 μm Si film deposited on a specially treated LB3-type Cu foil with a concavo-convex surface. Gowda et al. [25] reported a capacity of 0.42 mAh cm^{-2} at 0.9C over 70 cycles for a 1 μm Si on porous Ni current collector. By improving the adhesive force between the silicon film and current collector, the effect of volume changes of silicon on the stability of the system is reduced and high capacity can be retained even for very thick silicon films.

Various copper oxide nanostructures can be readily obtained through thermal [8,26] or hydrothermal [27] or anodic oxidation [27,28] of Cu foil, which represent promising candidates as high-loading matrix for thick Si film electrodes, because copper oxides, as a conversion type anode material for LIBs, can be completely reduced to metallic Cu at a relatively high potential (~0.7 V *vs*. Li/Li^+) [29,30]. Consequently, it is quite promising to use nanostructured Cu foil as matrix material to load thick Si films, which release most of its capacity at low potentials (<0.4 V *vs*. Li/Li^+) [4,22,31], while the electrochemically reduced Cu matrix is expected to collect currents and accommodate volume changes during discharge/charge processes.

Here we propose a feasible design to fabricate micrometer-scale silicon films deposited on nanostructured Cu foil as high capacity anodes for LIBs with excellent cycling performance. Hydrated copper oxides precursors were firstly produced by anodic oxidation of Cu foils in 1 M NaOH solution, which were then annealed in vacuum to obtain copper oxide nanofibers. Silicon films (1–2 μm) were afterwards deposited by e-beam evaporation. At low potentials, copper oxide nanofibers are in-situ reduced to metallic Cu nanofibers without damaging the structures, which work as electrical highways for fast electron transport and a reliable mechanical matrix to accommodate volume changes during lithium–silicon alloy/dealloy processes. Since copper oxide nanofibers were directly grown on Cu foil, the adhesion to the substrate is strong enough to support thick silicon, while avoiding the employment of conductive additives and polymer binders. The engineered thick Si film exhibits outstanding specific capacity and long cycle life. The 2 μm silicon film electrode can maintain a high capacity of 0.6 mAh cm^{-2} after 200 cycles at a current density of 0.225 mA cm^{-2}. The reported concept can be a general method for high-loading-film electrodes, which is industrial scalable and compatible with current battery manufacturing processes.

2. Experimental

2.1. Fabrication of Si-copper oxide nanofibers anode

Copper oxide nanofibers were obtained by a galvanostatic anodic oxidation of Cu foil followed by a heat treatment in vacuum. Before use, Cu foil (thickness of 25 μm, Goodfellow) was carefully cleaned with HCl, water and deionized water, and then one side of Cu foil was protected with adhesive tape to avoid being oxidized. A 2 × 3 cm Cu foil as working electrode, another Cu foil as counter electrode were immersed in 1 M NaOH solution. A constant current at the density of 1.5 mA cm^{-2} were applied onto the working electrode for 10 min. A faint blue coating on top of Cu foil were then obtained, which were hydrated copper oxides nanofibers. The sample was thoroughly cleaned in deionized water, heated under vacuum at 180 °C for one hour, and naturally cooled down to room temperature. Black copper oxide nanofibers were finally obtained. Since small amount of Cu^{2+} ions were introduced into NaOH solution and affected the load density of copper oxides, the NaOH solution after use were analyzed using Inductively Coupled Plasma (ICP, IRIS Intrepid II XUV, Thermo Fisher Scientific GmbH). And the concentration of Cu^{2+} ions was determined to be around 1 mM. The mass of copper oxides was determined by dissolving sample into 0.1 M HCl. The mean load density of copper oxide nanofibers is 0.675 mg cm^{-2}. 1 μm Si film (0.216 mg cm^{-2}) and 2 μm Si film (0.547 mg cm^{-2}) were afterwards deposited onto the copper oxide nanofibers using e-beam evaporation (BOC Edwards FL400, Germany). In order to determine the thickness of Si film, Si was firstly deposited on smooth silicon wafer and then measured by Profilometer Dektak XT (Brucker).

2.2. Characterization

The surface morphology of electrode was characterized by scanning electron microscopy (SEM, Zeiss DSM982). The composition of Si-copper oxide nanofibers anode was determined by X-ray diffraction (XRD, PANalyticalX'Pert PRO Diffraction, Co-Kα radiation, reflection geometry) and Raman spectroscopy (Renishaw) with 442 nm wavelength.

2.3. Electrochemical measurement

Electrochemical measurements were carried out using Swagelok-type cells assembled in an Ar-filled glove box (H_2O < 0.1 ppm, O_2 < 0.1 ppm, MBraun, Germany). Working electrodes were 1 cm discs directly punched from the copper oxide nanofibers-Si foil. Lithium foil was used as counter electrode, and a Whatman glass membrane was used as separator. The electrolyte was 1 M $LiPF_6$ dissolved in a mixture of ethylene carbonate/dimethyl carbonate/diethyl carbonate (EC/DMC/DEC; 1:1:1, by weight, Merck), including 2 wt% vinylene carbonate (VC) electrolyte additive (Merck). Zahner IM6 electrochemical workstation was used to measure cyclic voltammetry at a scan rate of 100 μV s^{-1}. Arbin BT2000 system was used to perform the galvanostatic

charge/discharge measurements. The weight values were obtained with a high precision electronic balance (Mettler Toledo).

3. Results and discussion

3.1. Materials characterization

Fig. 1a shows the XRD pattern of a 2 μm Si-film/copper oxide nanofibers on copper foil substrate. It reveals that the copper oxide nanofibers are a mixture of CuO and Cu_2O, which are consistent with the standard data of JCPDS 00-005-0661 and 00-002-1067, respectively. There are no signals from the silicon film, indicating that the Si film is amorphous. The Raman spectrum (Fig. 1b) of the 2 μm Si film on the copper oxide nanofibers shows broad peaks around 310 and 470 cm^{-1}, corresponding to the typical Raman vibration of amorphous silicon [32]. No signal arising from the underneath copper oxides was observed since Raman signal cannot reach such a depth.

The SEM images of Si-film/copper oxide nanofibers are shown in Fig. 2. The hydrated copper oxides precursors were produced by anodically oxidizing of Cu foil, and subsequently dehydrated into CuO/Cu_2O nanofibers after being vacuum annealed at 180 °C (Fig. 2a and b). The nanofibers are around 10 μm in length and 100 nm in diameter. Fig. 2b clearly reveals that copper oxide nanofibers possess adequate spaces in-between them, which is beneficial for the subsequent silicon deposition. Fig. 2c and d display the SEM images of the 1 μm Si film on the CuO/Cu_2O nanofibers, demonstrating that the silicon film was deposited along the nanofibers' length. Fig. 2e and f show the SEM images with 2 μm Si film loading. The originally narrow nanofibers grow into finger-like nanorods with 1 μm Si film loading, and the nanorods grow even wider and larger in size with 2 μm Si loading, tending to close up the gaps in-between them. The cross section images shown in the inset of Fig. 2e confirms that the silicon film was uniformly coated along the nanofibers' length.

3.2. Electrochemical performance

To verify the functions of the CuO/Cu_2O nanofibers, cyclic voltammetry (CV) measurements were conducted using pristine copper oxide nanofibers as anode in the potential window of 0.02–3.0 V at a scan rate of 100 μV s^{-1}. Fig. 3a shows that during the first discharge, four cathodic peaks can be observed at around 2.0, 1.2, 1.0 and 0.7 V, which correspond to multistep electrochemical reaction processes: the formation of a solid solution of $Cu^{II}_{1-x}Cu^{I}_{x}O_{1-x/2}$ ($0 \le x \le 0.4$), a phase transition into Cu_2O, then the formation of metallic Cu and Li_2O followed by the growth of an organic-type coating [29,30]. And three main anodic peaks are found around 1.2, 1.7 and 2.5 V, corresponding to the gradual delithiation processes. In the subsequent cycles, the main cathodic peaks are observed at around 2.5, 1.3 and 1.1 V as well as a smooth peak range of 0.7–0.5 V, while the anodic peaks are highly overlapped with these of the first cycle. Therefore, only metallic Cu nanofibers exist at the reactive potentials of Si anode (<0.4 V). Another CV measurement was carried out in the potential window of 0.02–1.0 V for the pristine copper oxide anodes as well. Fig. 3b shows that the faradaic current has disappeared, occurring only the capacitive current. This means the redox reaction of copper oxides are restricted in the potential window of 0.02–1.0 V. After the coating of Si film, copper oxide nanofibers are not exposed to the electrolyte, further restraining the capacitive contribution.

CV measurements for 2 μm Si–CuO/Cu_2O nanofibers anode were conducted at 100 μV s^{-1} in the potential window of 0.02–1.0 V, which restrains the oxidation of metallic copper. The result in Fig. 3c shows the typical amorphous silicon lithiation/delithiation processes. One small cathodic peak is found at 0.83 V during the first discharge, which could be attributed to both the formation of solid-electrolyte-interphase (SEI) layer and the complete reduction of CuO into metallic Cu (the peak at 0.7 V shown in Fig. 3a). This peak disappears during the subsequent scans, indicating that the copper did not participate in the reactions. This is confirmed by galvanostatic discharge/charge measurements in Fig. 3d, where the sloping pseudo-plateau extending from 0.8 V to 0.7 V in the first discharge process disappears in the subsequent cycles. The major cathodic peak starts from around 0.4 V–0 V during the first discharge and then splits into two peaks (0.18 V, 0 V) in the subsequent cycles, which is consistent with typical lithiation behaviors of amorphous Si film [31]. Two anodic peaks are observed around 0.35, 0.5 V in the first charge process and retain nearly the same positions in the second and third scans, both of which correspond to the extraction of lithium from silicon. No signal arising from the oxidation of copper is observed, which explains why no copper oxides participate in the following discharges. From the above discussion, we can conclude that during the first discharge (after 0.7 V), copper oxides were electrochemically reduced into metallic copper, afterwards they only work as mechanical and electrical support for the silicon lithiation/delithiation. In the subsequent scans, lithium only reacts with silicon, which contributes the whole capacity.

Fig. 3d displays representative discharge-charge voltage profiles of the 2 μm Si–CuO/Cu_2O nanofibers anodes for the first five cycles at a current rate of 0.45 mA cm^{-2} in a potential window of 0.02–1.0 V, with the exception of a window 0.02–3.0 V for the first discharge. The first discharge has four sloping ranges (2.0–1.8, 1.3–1.2, 1.2–1.1 and 0.8–0.7 V) for the reduction of copper oxides, and a long plateau from 0.35 V to 0.02 V for the lithiation of silicon,

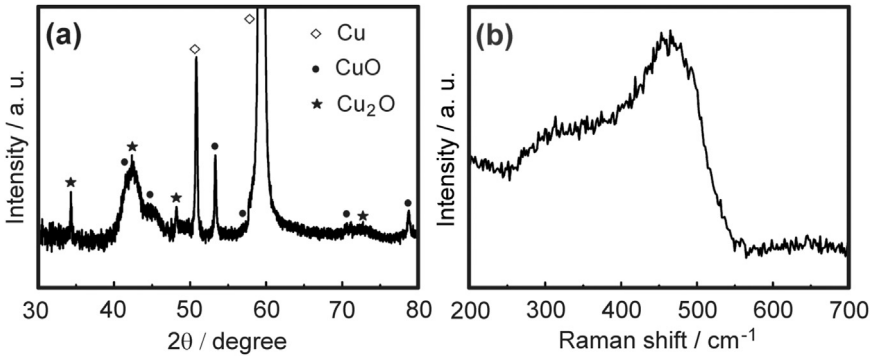

Fig. 1. (a) XRD pattern, (b) Raman spectrum of 2 μm Si on copper oxide nanofibers.

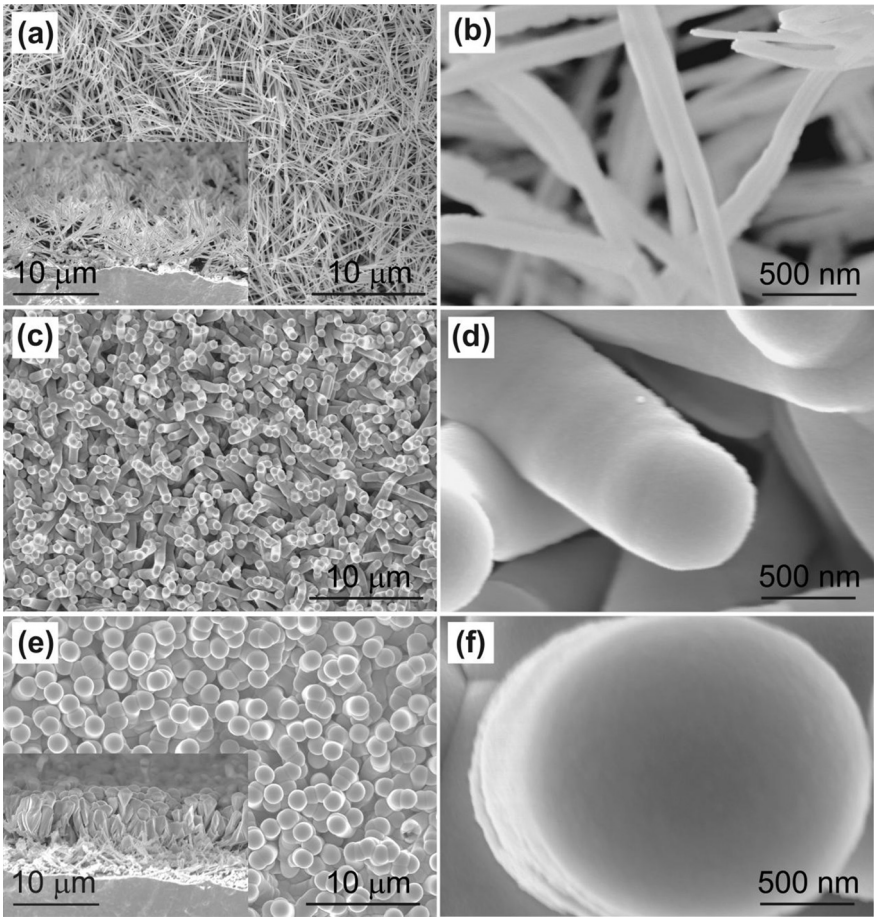

Fig. 2. SEM images with low and high magnifications: (a–b) CuO/Cu_2O nanofibers, (c–d) 1 μm Si film on CuO/Cu_2O nanofibers, (e–f) 2 μm Si film on CuO/Cu_2O nanofibers.

while the first charge process includes two sloping ranges (more evident at low current rates in Fig. 3e), which are consistent with CV results. The first discharge/charge profiles deliver total capacities of 1.74 mAh cm^{-2}/0.97 mAh cm^{-2}, respectively, while the reduction of copper oxides contributes only 0.19 mAh cm^{-2} to the total capacity. In this work, for the ease of comparing with the subsequent cycles, we only consider the capacities contributed by the lithiation/delithiation of Si film. Thus we have an initial discharge capacity of 1.55 mAh cm^{-2} (2830 mAh g^{-1}) and a Coulombic efficiency of 62.6%. Remarkably, the Coulombic

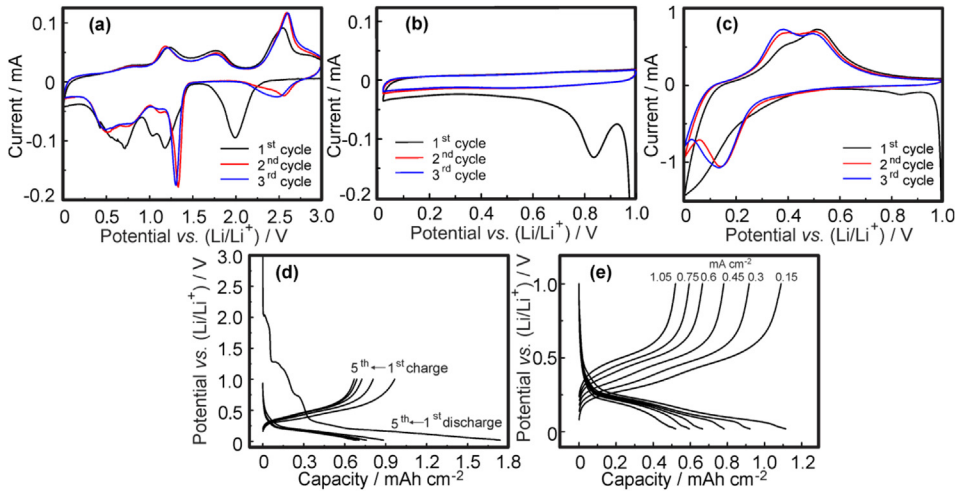

Fig. 3. CV profiles at a scan rate of 100 μV s^{-1} (a) in the potential window of 0.02–3.0 V, (b) in 0.02–1.0 V for pristine CuO/Cu_2O nanofibers anode, (c) in the potential window of 0.02–1.0 V for 2 μm Si–CuO/Cu_2O nanofibers anode. (d) Discharge-charge voltage profiles of the 2 μm Si–CuO/Cu_2O nanofibers anode for the first five cycles at a current density of 0.45 mA cm^{-2} in the potential range of 0.02–1.0 V, with the exception of a potential window 0.02–3.0 V for the first discharge. (e) Representative discharge-charge voltage profiles at various current densities from 0.15 mA cm^{-2} to 1.05 mA cm^{-2}.

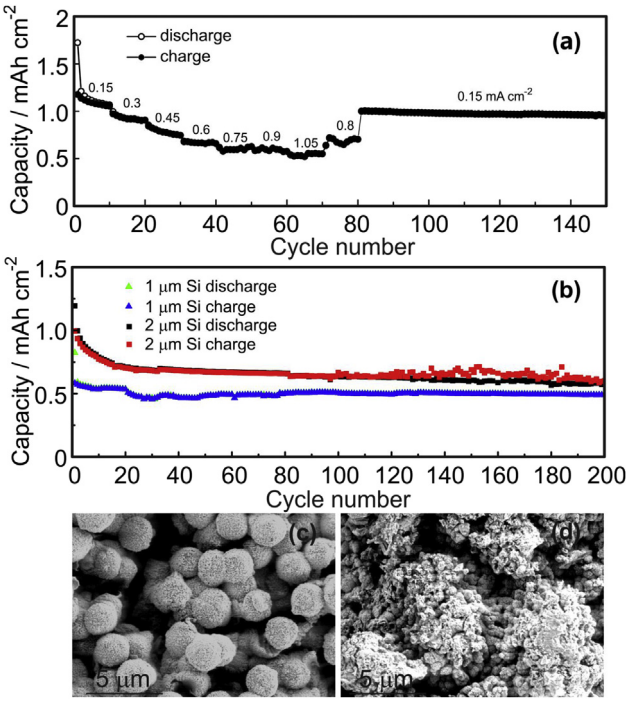

Fig. 4. (a) Rate performance of 2 μm Si–CuO/Cu_2O nanofibers anode over a potential window of 0.02–1.0 V under varying current rates from 0.15 to 1.05 mA cm^{-2}. (b) Electrochemical cycling performance over a potential window of 0.02–1.0 V under a current density of 0.225 mA cm^{-2} for 200 cycles for 1–2 μm Si–CuO/Cu_2O nanofibers anode. The 2 μm Si–CuO/Cu_2O nanofibers sample was firstly tested for three cycles of CV measurement. SEM images of 2 μm Si– CuO/Cu_2O nanofibers after (c) two cycles and (d) 200 cycles.

efficiency steadily reaches a value higher than 99.0% after 7 cycles (see Fig. 5a).

It is expected that the use of electrochemically in-situ reduced metallic Cu nanofibers as efficient electron pathways and mechanical matrix for silicon film leads to further improvements in the rate capability. The representative discharge-charge voltage profiles of a 2 μm Si–CuO/Cu_2O nanofibers anode at various rates

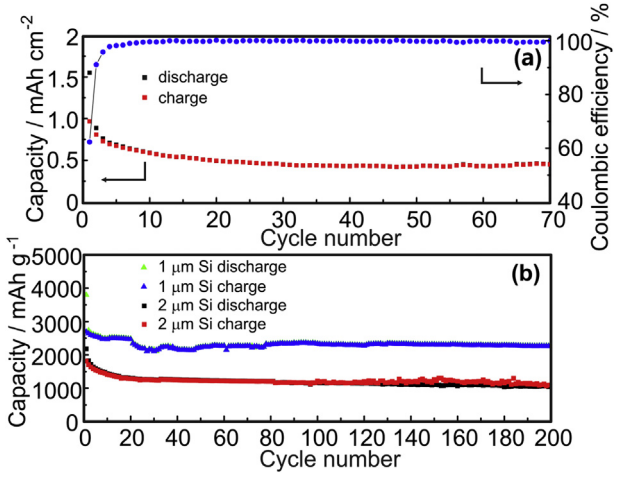

Fig. 5. (a) Electrochemical cycling performance over a potential window of 0.02–1.0 V at a current density of 0.45 mA cm^{-2} for 70 cycles for 2 μm Si–CuO/Cu_2O nanofibers anode. (b) Electrochemical cycling performance with the gravimetric units over a potential window of 0.02–1.0 V at a current density of 0.225 mA cm^{-2} for 200 cycles for 1 and 2 μm Si–CuO/Cu_2O nanofibers anode.

are shown in Fig. 3e. At a high current rate of 1.05 mA cm^{-2}, a sloping pseudo-plateau ranging from 0.3 to 0.02 V is still clearly seen from the discharge profile, implying excellent rate performance. The electrons generated from the lithiation reaction of silicon can be effectively transported to the current collector even at a high discharge/charge current rate. The in-situ reduced metallic Cu nanofibers are directly connected to the current collector, which work as electrical highways for fast electron transport, thus enabling the outstanding rate capability. The rate capability (Fig. 4a) was measured over 150 cycles at various current rates ranging from 0.15 mA cm^{-2} to 1.05 mA cm^{-2}. The discharge capacities are 1.098, 0.921, 0.776, 0.665, 0.595, 0.582 and 0.519 mAh cm^{-2} at 0.15, 0.3, 0.45, 0.6, 0.75, 0.8, 0.9 and 1.05 mA cm^{-2}, respectively. Remarkably, even after cycling at a high rate of 1.05 mA cm^{-2} (i.e., 1.92 A g^{-1}), the capacity is still able to recover to the initial value of around 1 mAh cm^{-2} (1827 mAh g^{-1}) when the current rate is set back to 0.15 mA cm^{-2}. After 150 cycles, the reversible capacity can still maintain as high as 0.95 mAh cm^{-2}. Cao et al. [8] have reported a 500 nm-Si film can retain a specific capacity of 790 mAh g^{-1} (around 0.095 mAh cm^{-2}) upon a high current rate of 14 A g^{-1} (around 1.7 mA cm^{-2}). Gowda et al. [25] achieved a reversible capacity of 0.6 mAh cm^{-2} at 0.2C with a 2 μm Si film. Compared with these results, we could conclude that the 2 μm Si–CuO/Cu_2O nanofibers anode in this work demonstrates a superior rate capability.

The long-term cycling stability was examined at a current density of 0.225 mA cm^{-2}. The 1 μm Si–CuO/Cu_2O nanofibers anode (Fig. 4b) exhibits an initial discharge capacity of 0.822 mAh cm^{-2} (3798 mAh g^{-1}) and a charge capacity of 0.583 mAh cm^{-2} (2693 mAh g^{-1}). The specific capacity with the gravimetric units can be found in Fig. 5b. Since the formation of SEI layer consumes a certain percentage of lithium, the Coulombic efficiency of the first cycle is 70.9%, but it increases to 96% in the second cycle and finally remains as high as 99% after seven cycles. After 200 cycles, a capacity of 0.48 mAh cm^{-2} (2222 mAh g^{-1}) is still retained, which is 82.5% of its initial charge capacity and higher than that for previously reported Si films [8,25]. For the 2 μm Si–CuO/Cu_2O nanofibers anode, the initial discharge/charge capacities are 1.193 mAh cm^{-2} (2179 mAh g^{-1})/0.994 mAh cm^{-2} (1816 mAh g^{-1}), respectively, resulting in a Coulombic efficiency of 83.3%. After 200 cycles, a high specific capacity of 0.6 mAh cm^{-2} (1096 mAh g^{-1}) is retained, which is 60.4% of its initial charge capacity. Since the in-situ electrochemically reduced metallic Cu nanofibers were directly grown on Cu foil, the adhesion to the substrate is strong enough to support thick silicon, ensuring good long-term cycling stability. The SEM images after cycling are shown in Fig. 4c and d. After shallow cycling (two cycles), the original smooth surface exhibits a large amount of wrinkles due to the strain introduced during discharge/charge. While after deep cycling, the Si surface has experienced dramatic changes. Small wrinkles have evolved into agglomerated small particles, and still keep in close contact with each other.

The active Si loading density plays an important role in determining the overall capacity of Si electrodes for LIBs. Si thin films usually exhibit very high specific capacities for a thickness less than 500 nm, which is realized actually at the expense of low loading density. In this work, the 2 μm Si film achieved a considerably high capacity, attributed to the nanostructured Cu foil. It is clearly demonstrated herein that normal Cu foil decorated with nanostructured copper oxides, which could be in-situ reduced to metallic Cu nanofibers, could work as advanced current collector for loading silicon and further be used as promising anode in LIBs. Based on this point, we still hold promise of further increasing the thickness of Si film while maintaining a high specific capacity and long cycling life in future work.

4. Conclusion

In conclusion, we have presented a new concept to fabricate binder-free thick silicon films on pre-anodically oxidized Cu foil as high capacity anode for LIBs. The silicon film exhibits impressive cycling performance and rate capability due to nanostructured Cu foil which offers both the strong adhesion and fast electron transport for silicon. After 200 cycles discharge/charge at a current density of 0.225 mA cm^{-2}, high reversible capacities of 0.48 mAh cm^{-2} (2222 mAh g^{-1}) and 0.6 mAh cm^{-2} (1096 mAh g^{-1}) are retained for the 1 μm silicon film electrode and the 2 μm silicon film electrode, respectively. After cycling at high current rates, the 2 μm silicon film electrode is still able to recover to the initial value of around 1 mAh cm^{-2} (1827 mAh g^{-1}) when the current rate is set back to 0.15 mA cm^{-2}, demonstrating excellent rate capability. Our work clearly demonstrates that a Cu foil decorated with nanostructured copper oxides could work as advanced current collector for high-loading silicon and further be used as promising thin film anode for high performance LIBs.

Acknowledgments

This work was financed by the International Research Training Group (IRTG) project and PAKT project “Electrochemical energy storage in autonomous systems, no. 49004401”. We thank Ronny Engelhard for technical support, Dr. Stefan Baunack for SEM imaging help, Xueyi Lu for discussions, Andrea Voß for ICP measurement. C.Yan acknowledges the support from the "Thousand Talents Program" and the Priority Academic Program Development of Jiangsu Higher Education Institutions (PAPD).

References

[1] J.P. Maranchi, A.F. Hepp, P.N. Kumta, Electrochem. Solid State Lett. 6 (2003) A198–A201.
[2] M.N. Obrovac, L. Christensen, Electrochem. Solid State Lett. 7 (2004) A93–A96.
[3] J. Li, J.R. Dahn, J. Electrochem. Soc. 154 (2007) A156–A161.
[4] T.D. Hatchard, J.R. Dahn, J. Electrochem. Soc. 151 (2004) A838–A842.
[5] M.N. Obrovac, L.J. Krause, J. Electrochem. Soc. 154 (2007) A103–A108.
[6] C. Liu, F. Li, L.-P. Ma, H.-M. Cheng, Adv. Mater. 22 (2010) E28–E62.
[7] S. Guo, H. Li, H. Bai, Z. Tao, J. Chen, J. Power Sources 248 (2014) 1141–1148.
[8] F. Cao, J. Deng, S. Xin, H. Ji, O.G. Schmidt, L. Wan, Y. Guo, Adv. Mater. 23 (2011) 4415–4420.
[9] W. Ren, C. Wang, L. Lu, D. Li, C. Cheng, J. Liu, J. Mater. Chem. A 1 (2013) 13433–13438.
[10] W.-J. Zhang, J. Power Sources 196 (2011) 13–24.
[11] C.K. Chan, H. Peng, G. Liu, K. Mcllwarth, X.F. Zhang, R.A. Huggins, Y. Cui, Nat. Nanotechnol. 3 (2008) 31–35.
[12] H. Wu, G. Chan, J.W. Choi, I. Ryu, Y. Yao, M.T. McDowell, S.W. Lee, A. Jackson, Y. Yang, L. Hu, Y. Cui, Nat. Nanotechnol. 7 (2012) 310–315.
[13] Y. Yao, M.T. McDowell, I. Ryu, H. Wu, N. Liu, L. Hu, W.D. Nix, Y. Cui, Nano Lett. 11 (2011) 2949–2954.
[14] H. Li, X.J. Huang, L.Q. Chen, Z.G. Wu, Y. Liang, Electrochem. Solid-State Lett. 2 (1999) 547–549.
[15] Y. Park, N.-S. Choi, S. Park, S.H. Woo, S. Sim, B.Y. Jang, S.M. Oh, S. Park, J. Cho, K.T. Lee, Adv. Energy Mater. 3 (2013) 206–212.
[16] X. Zhao, C.M. Hayner, M.C. Kung, H.H. Kung, Adv. Energy Mater. 1 (2011) 1079–1084.
[17] J. Deng, H. Ji, C. Yan, J. Zhang, W. Si, S. Baunack, S. Oswald, Y. Mei, O.G. Schmidt, Angew. Chem. Int. Ed. 52 (2013) 2326–2330.
[18] H. Kim, M. Seo, M.-H. Park, J. Cho, Angew. Chem. Int. Ed. 49 (2010) 2146–2149.
[19] H. Wu, G. Yu, L. Pan, N. Liu, M.T. McDowell, Z. Bao, Y. Cui, Nat. Commun. 4 (2013) 1943.
[20] S. Ohara, J. Suzuki, K. Sekine, T. Takamura, J. Power Sources 136 (2004) 303–306.
[21] T. Moon, C. Kim, B. Park, J. Power Sources 155 (2006) 391–394.
[22] S. Bourderau, T. Brousse, D.M. Schleich, J. Power Sources 81-82 (1999) 233–236.
[23] T. Takamura, M. Uehara, J. Suzuki, K. Sekine, K. Tamura, J. Power Sources 158 (2006) 1401–1404.
[24] J. Yin, M. Wada, K. Yamamoto, Y. Kitano, S. Tanase, T. Sakai, J. Electrochem. Soc. 153 (2006) A472–A477.
[25] S.R. Gowda, V. Pushparaj, S. Herle, G. Girishkumar, J.G. Gordon, H. Gullapalli, X. Zhan, P.M. Ajayan, A.L.M. Reddy, Nano Lett. 12 (2012) 6060–6065.
[26] X.C. Jiang, T. Herricks, Y.N. Xia, Nano Lett. 2 (2002) 1333–1338.
[27] J. Juodkazyte, B. Sebeka, I. Savickaja, A. Selskis, V. Jasulaitiene, P. Kalinauskas, Electrochim. Acta 98 (2013) 109–115.
[28] X. Wu, H. Bai, J. Zhang, F.e. Chen, G. Shi, J. Phys. Chem. B 109 (2005) 22836–22842.
[29] A. Débart, L. Dupont, P. Poizot, J.-B. Leriche, J.M. Tarascon, J. Electrochem. Soc. 148 (2001) A1266–A1274.
[30] F. Ke, L. Huang, G. Wei, L. Xue, J. Li, B. Zhang, S. Chen, X. Fan, S. Sun, Electrochim. Acta 54 (2009) 5825–5829.
[31] K.-L. Lee, J.-Y. Jung, S.-W. Lee, H.-S. Moon, J.-W. Park, J. Power Sources 129 (2004) 270–274.
[32] A.T. Voutsas, M.K. Hatalis, J. Boyce, A. Chiang, J. Appl. Phys. 78 (1995) 6999–7006.